valuable suggestions.

References

1. Binns, A. N.; Thomashaw, M. F. *Annu. Rev. Microbiol.* **1988**, *42*, 575.
2. Bourret, R. B.; Borkovich, K. A.; Simon, M. I. *Annu. Rev. Biochem.* **1991**, *60*, 401.
3. Lee, K.; Dudley, M. W.; Hess, K. M.; Lynn, D. G.; Joerger, R. D.; Binns, A. N. *Proc. Natl. Acad. Sci. USA* **1992**, *89*, 8666.
4. Boulton, G. W.; Nester, E. W.; Gordon, M. P. *Science* **1986**, *232*, 983.
5. Spencer, P. A.; Towers, G. H. N. *Phytochemistry* **1988**, *27*, 2781.
6. Melchers, L. S.; Regensburg-Tuink, A. J. G.; Schilperoot, R. A.; Hooykaas, P. J. *J. Mol. Microbiol.* **1989**, *3*, 969.
7. Schreuder, H. A.; Prick, P. A. J.; Wierenga, R. K.; Vriend, G.; Wilson, K. S.; Hol, W. G. J.; Drenth, J. *J. Mol. Biol.* **1989**, *208*, 679.
8. Hess, K. M.; Dudley, M.W.; Lynn, D. G.; Joerger, R. D.; Binns, A. N. *Proc. Natl. Acad. Sci. USA* **1991**, *88*, 7854.
9. Hartman, F. C. *Biochem. Biophys. Res. Comm.* **1968**, *33*, 888.
10. Benson, S. W.; Cruickshank, F. R.; Golden, D. M.; Haugen, G. R.; O'Neal, H. E.; Rogers, A. S.; Shaw, R.; Walsh, R. *Chem. Rev.* **1969**, *69*, 279.
11. Hess, K. M. *Initiation of signal transduction pathways by phenolics in plants and bacteria*; Ph.D. Thesis, The University of Chicago, 1991.
12. Perrin, D. D.; Boyd, D.; Sergeant, E. P. *pKa prediction for organic acids and bases*; Chapman and Hall Press, 1981.
13. Lee, K.; Tzeng, Y.-L.; Liu, N.; Dudley, M. W.; Lynn, D. G. *Pure & Appl. Chem.* **1993**, *65*, 1241.
14. Spencer, P. A.; Tower, G. H. N. *Phytochemistry* **1988**, *27*, 2781.
15. Dudley, M. *Synthetic probes of signal transduction pathways*; Ph.D. Thesis, The University of Chicago, 1991.
16. Zeng, Z. Cycloprpylquinone: A probe of redox processes in development and a substrate for a unique photoannulation reaction; Ph.D. Thesis, The University of Chicago, 1994.
17. Chilton, M. D.; Currier, T.; Farrand, S.; Bendich, A.; Gordon, M.; Nester, E. W. *Proc. Natl. Acad. Sci. USA* **1974**, *71*, 3672.
18. Stachel, S. E.; Nester, E. W. *EMBO J.* **1986**, *5*, 1445.

Sharp-Line Electronic Spectroscopy and Ligand Field Analysis of [Cr(*trans*-diammac)](ClO$_4$)$_3$[1]

Jong-Ha Choi* and In-Gyung Oh

Department of Chemistry, Andong National University, Andong 760-749, Korea
Received August 13, 1996

The luminescence and excitation spectra of [Cr(*trans*-diammac)](ClO$_4$)$_3$ (*trans*-diammac=*trans*-6,3-dimethyl-1,4,8,11-tetraazacyclotetradecane-6,13-diamine) taken at 77 K are reported. The mid and far-infrared spectra at room-temperature are also measured between 4000 cm^{-1} and 50 cm^{-1}. In the excitation spectrum the ^2E_g components are splitted by 102 cm^{-1}. Using the observed electronic transitions, a ligand field analysis was performed to determine more detailed bonding properties of the coordinated atoms toward chromium(III). According to the results, we can confirm that the six nitrogen atoms have a strong σ-donor character, and the *trans*-diammac secondary amine has a greater value of e_σ than does the primary amine.

Introduction

The sharp-line spectroscopic study of chromium(III) compound started with six coordinated nitrogen atoms, because the intensities of absorption or excitation spectra at the low temperature of these compound are very strong. In recent years a considerable amount of such spectral data has been accumulated.[2-5] The ligand field optimization of the electronic spectra, including the sharp spin-forbidden transitions promises to provide more detailed information concerning metal-ligand interactions.[6-10] With the use of chromium(III) system, the sharp electronic lines can be found with a precision two orders of magnitude greater than the broad spin-allowed bands. The sharp-line splittings are also quite sensitive to the metal-ligand geometry. Thus, it is possible to extract geometric information from the molecular spectroscopy.[11-13]

There has also been considerable interest in the coordination chemistry of the pendant arm macrocyclic hexaamine ligand, 6,3-dimethyl-1,4,8,11-tetraazacyclotetradecane-6,13-diamine (diammac) with the first row transition metal ions.[14-17] The syntheses and structural characterization of chromium(III) complexes with *trans* and *cis* ligand conformations (Figure 1) have been reported.[16,17] It was found

that these ligands can form very stable complexes due to their strong chelating effect. The *trans* isomer contrasts with *cis* isomer in showing very unusual spectroscopic and structural properties, for examples, the electronic maxima are shifted to higher energy compared with those of other hexaamines, and Cr-N bonds are the shortest reported for a number of CrN_6^{3+} compounds.[17]

In this study the 77 K luminescence and excitation spectra, and the room-temperature infrared and UV-visible spectra of [Cr(*trans*-diammac)]$(ClO_4)_3$ were measured. The seven electronic origins were assigned by analyzing the absorption and excitation spectra. Using the observed electronic transitions, a ligand field analysis was performed to determine more detailed bonding properties for the primary and secondary nitrogen atoms of *trans*-diammac toward chromium(III).

Experimental

The synthetic method of [Cr(*trans*-diammac)]$(ClO_4)_3$ has been reported.[17] The microcrystalline samples were generously supplied by Professor Geoffrey A. Lawrance. The compound was recrystallized three times for spectroscopic measurements.

The room-temperature visible spectrum was recorded with a Hewlett-Packard 8452A diode array spectrophotometer. The mid-infrared spectrum was obtained with a Bomen michelson 100 spectrometer on a CsI pellet. The far-infrared spectrum in the region 650-50 cm^{-1} was recorded with a Bruker 113v spectrometer with sample in polyethylene. The luminescence and excitation spectra were measured at 77 K with a Spex Fluorolog-2 FL212 spectrofluorometer as described previously.[3]

All optimizations and calculations for the ligand field parameterization were performed on an IBM mainframe computer. Some simple computations and data manipulations were done on an IBM-compatible Pentium 166 MHz microcomputer with a 32 MB main memory.

Results and Discussion

Vibrational Intervals. An experimental problem lies with the difficulty in distinguishing pure electronic components from the vibronic bands that also appear in the sharp-line absorption or excitation spectra. It is required the vibrational intervals due to the electronic ground state be obtained by comparing the luminescence spectrum with infrared data. Figures 2 and 3 represent the mid and far-infrared spectra of [Cr(*trans*-diammac)]$(ClO_4)_3$ recorded at room-temperature.

The strong peaks at 841 and 786 cm^{-1} are primarily involved in the NH_2 and CH_2 rocking modes, respectively. The very strong sharp band at 625 cm^{-1} has been attributed to perchlorate ion. The Cr-N stretching bands were detected in the range 420-490 cm^{-1}. A number of absorption bands below 328 cm^{-1} arise from ring deformations and lattice vibrations.

The 427 nm excited 77 K luminescence spectrum of [Cr(*trans*-diammac)]$(ClO_4)_3$ is also shown in Figure 4. The band positions relative to the lowest zero-phonon line, with corresponding infrared frequencies, are listed in Table 1. The luminescence spectrum was independent of the exciting wavelength within the first spin-allowed transition region.

The strongest peak, at 14698 cm^{-1}, is assigned as the zero-phonon line, R_1, because a corresponding strong peak is found at 14700 cm^{-1} in the excitation spectrum. A well defined hot band at 14798 cm^{-1} may be assigned to the second component of the $^2E_g \rightarrow {}^4A_{2g}$ transition. The vibronic intervals occurring in the spectrum consist of several modes those can be presumed to involve primarily ring torsion and angle-bending modes with frequencies in the range 133-379

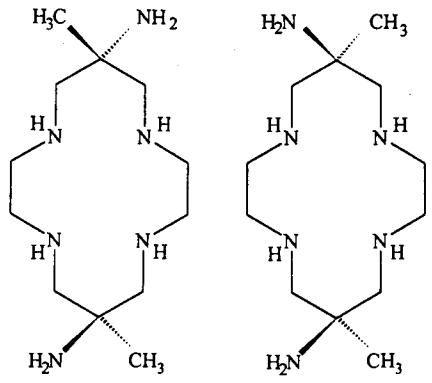

Figure 1. Two possible geometric isomers of diammac ligand.

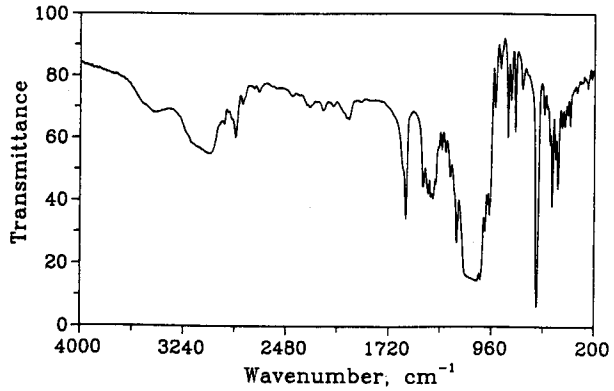

Figure 2. Mid-infrared spectrum of [Cr(*trans*-diammac)]$(ClO_4)_3$ at 298 K.

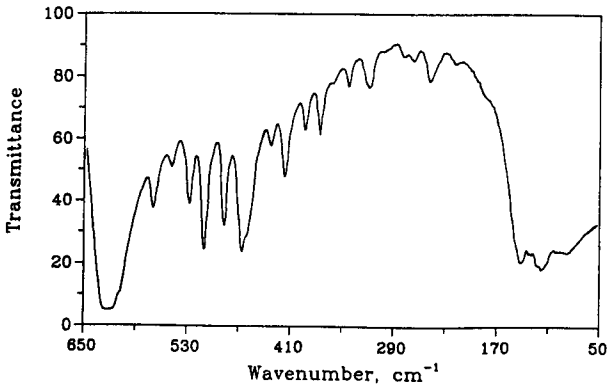

Figure 3. Far-infrared spectrum of [Cr(*trans*-diammac)]$(ClO_4)_3$ at 298 K.

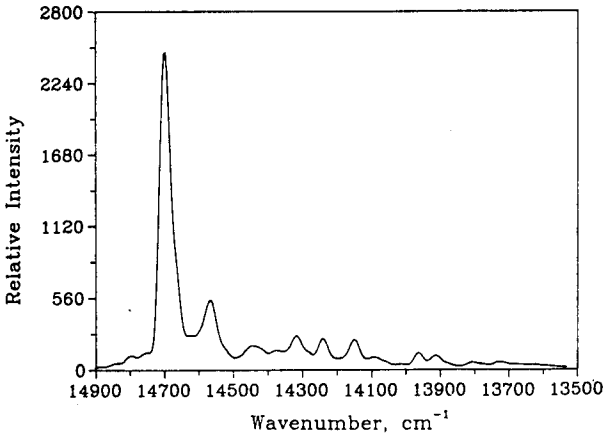

Figure 4. The 77 K luminescence spectrum of [Cr(*trans*-diammac)](ClO$_4$)$_3$ (λ_{ex}=427 nm).

Table 1. Vibrational Frequencies from the 77 K Luminescence and 298 K Infrared Spectra for [Cr(*trans*-diammac)](ClO$_4$)$_3$[a]

Luminescence[b]	Infrared	Assignment
−140 vw		
−100 m		R_2
0 vs		R_1
69 w	75 vw	Lattice vib.
133 s	118 m, 142 m	and
251 w	220 vw, 250 w	δ (N-Cr-N)
325 vw	328 w	
379 s	378 m, 397 w	ν(Cr-N$_{prim}$)
	420 w	
456 s	438 w	ν(Cr-N$_{sec}$)
	471 s, 489 m	and
545 s	513 vs, 528 w	Ring def.
	571 m	
605 w	625 vs	ClO_4^-
684 vw		113+545
735 m	733 vs	
785 m	786 s	325+456
	894 m	ρ(CH$_2$)
	841 s	ρ(NH$_2$)
889 w	894 m	438+456
	934 m	
972 w	975 s	456+513
1021 vw	1011 m	471+545
	1042 s	

[a]Data in cm^{-1}. [b]Measured from zero-phonon line at 14697 cm^{-1}.

cm^{-1}. The band at 456 cm^{-1} can be assigned as a Cr-N stretching mode. It is well known that complexes with CrN_6 skeletons exhibit the strong absorption at this far infrared range.[3]

Electronic Transitions. Six-coordinated chromium (III) complexes exhibit three spin-allowed transitions from the ground state $^4A_{2g} \rightarrow {}^4T_{2g}$ (F) (ν_1), $^4T_{1g}$ (F) (ν_2) and $^4T_{1g}$ (P) (ν_3) in O_h notation. The third band, ν_3, usually occurs above 30000 cm^{-1} and would be obscured by ligand or charge-transfer absorption in this region. The UV-visible absorption spectrum exhibits two bands, one at 23390 cm^{-1} (ν_1) and the other at 29980 cm^{-1} (ν_2), corresponding to the $^4A_{2g} \rightarrow$

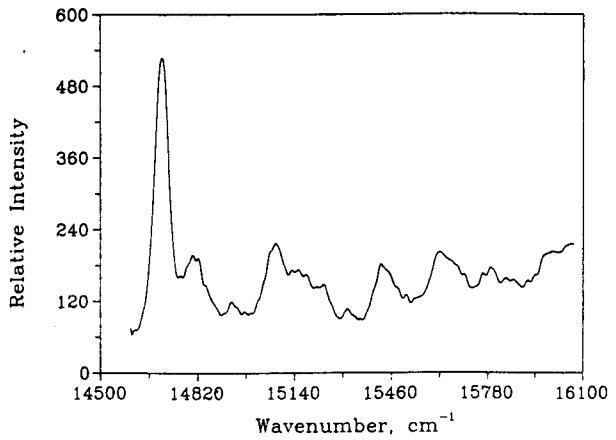

Figure 5. The 77 K excitation spectrum of [Cr(*trans*-diammac)](ClO$_4$)$_3$ (λ_{em}=707 nm).

$^4T_{2g}$ and $^4A_{2g} \rightarrow {}^4T_{1g}$ (O_h) transitions, respectively. The positions of these bands are different from those observed for other octahedral $[CrN_6]^{3+}$ complexes.[2-9] It is concluded that the shift in the first maximum to higher energy reflects a strong coordination of the diammac ligand. A clear splitting of the two quartet bands can not be detected. However, in order to have some point of reference for the splittings of the bands, we have fit the band profiles to four Gaussian curves. The contribution from the bands in the UV region was corrected. A deconvolution procedure on the experimental band pattern yields maxima at 22570, 24635, 29160, and 30620 cm^{-1} for the tetragonal splittings of $^4T_{2g}$ and $^4T_{1g}$, respectively. We used the average peak positions as the experimental transition energies. In general, using just one Gaussian curve instead of two yields a least-squares error only four times that of the best fit.

The 77 K excitation spectrum is shown in Figure 5. It was recorded by monitoring a relatively strong vibronic peak in the luminescence spectrum. The spectrum obtained was independent of the vibronic peak used to monitor it. The peak positions and their assignments are tabulated in Table 2. The calculated frequencies in parentheses were obtained by using the vibrational modes ν_1-ν_4 listed in Table 2.

Two strong peaks at 14700 and 14802 cm^{-1} in the excitation spectrum coincide with the luminescence spectrum are assigned to the two components (R_1 and R_2) of the $^4A_{2g} \rightarrow {}^2E_g$ transition. The lowest-energy zero-phonon line coincides with the luminescence origin within 2 cm^{-1}. In the excitation spectrum the ^2E_g splitting is found as a 102 cm^{-1}, and it is the largest which can be compared with those of the multidentate amine chromium(III) complexes.[5] In general, it is not easy to locate positions of the other electronic components because the vibronic sidebands of the ^2E_g levels overlap with the lines of $^2T_{1g}$. However, the three components of the $^4A_{2g} \rightarrow {}^2T_{1g}$ electronic origin (T_1, T_2 and T_3) can be found with strong intensities at 537, 725 and 920 cm^{-1} from the lowest electronic line, R_1. Vibronic satellites based on these origins also have similar frequencies and intensity patterns to those of the ^2E_g components.

Ligand Field Analysis. The ligand field potential matrix was assumed to arise only from the six coordinated nitrogen atoms. Although the perchlorate oxygens may also

Table 2. Assignment of Sharp-Line Positions in the 77 K Excitation Spectrum of [Cr(*trans*-diammac)]$(ClO_4)_3$[a]

$\bar{\nu}_0$-14700		Assignment	(Calcd)[b]		Vibronic frequencies[c]	Ground state frequencies[d]
0	vs	R_1		ν_1	81	69
102	s	R_2		ν_2	127	133
121	m	$R_1+\nu_2$	(127)	ν_3	377	379
208	vw	$R_1+\nu_1+\nu_2$	(208)	ν_4	446	456
230	m	$R_2+\nu_2$	(229)			
358	m	$R_2+2\nu_2$	(356)			
376	s	$R_1+\nu_3$	(377)			
431	w					
452	w	$R_1+\nu_4$	(446)			
479	w	$R_2+\nu_3$	(479)			
537	m	T_1	(548)			
616	m	$T_1+\nu_1$	(618)			
725	s	T_2				
809	w	$T_2+\nu_1$	(806)			
920	s	T_3				
1001	sh	$T_3+\nu_1$	(1001)			
1065	w	$T_3+\nu_2$	(1047)			
1090	m	$T_3+\nu_3$	(1102)			
1140	w					
1165	w	$T_2+\nu_4$	(1171)			
1213	w					
1241	w	$T_2+\nu_1+\nu_4$	(1252)			
1300	vw	$T_3+\nu_3$	(1297)			
1359	sh	$T_3+\nu_4$	(1366)			

[a]Data in cm^{-1}. [b]Values in parentheses represent the calculated frequencies based on the vibrational modes listed. [c]From the excitation spectrum. [d]From the luminescence spectrum.

perturbate metal *d* orbitals, the extent of that interaction was judged too small to warrant any additional adjustable parameters. The angular positions of coordinated nitrogens were taken from the X-ray crystal structure[17] of [Cr(*trans*-diammac)]$(ClO_4)_3$, which was determined to be monoclinic with the space group $P2_1/c$. The coordinates were then rotated so as to maximize the projections of the six-coordinated nitrogen atoms on the Cartesian axes centered on the chromium. The resulting Cartesian and spherical coordinates are shown in Table 3.

The ligand field analysis was carried out through an optimized fit of experimental to calculated transition energies. Hoggard[7] has described the methods for determining the eigenvalues and eigenfunctions of a d^3 ion in a ligand field from any number of coordinated atoms. The full set of 120 single-term antisymmetrized product wavefunctions was employed as a basis. The Hamiltonian we have used in the calculation was

$$\hat{H} = \sum_{i<j} \frac{e^2}{r_{ij}} + V_{LF} + \zeta \sum_i \boldsymbol{l}_i \cdot \boldsymbol{s}_i + \alpha_T \sum_i \boldsymbol{l}_i^2 + 2\alpha_T \sum_{i<j} \boldsymbol{l}_i \cdot \boldsymbol{l}_j \qquad (1)$$

the terms of which represent, the interelectronic repulsion, ligand field potential, and spin-orbit coupling, respectively with the last two representing the Trees correction.[18] The parameters varied during the optimization were the interelectronic repulsion parameters *B*, *C* and the Trees correction parameter α_T, the spin-orbit coupling parameter ζ, plus the AOM parameters, $e_s(N_{prim})$ for a primary amine-chromium, and $e_\sigma(N_{sec})$ for a secondary amine-chromium. The π-interaction of a nitrogen with sp^3 hybridization was assumed to be negligible. However, it is noteworthy that the peptide nitrogen with sp^2 hybridization has a weak π-donor character.[19] The six parameters were used to fit experimental energies: the five $^4A_{2g} \rightarrow \{^2E_g, {}^2T_{1g}\}$ components, identified in Table 4, the average energies of the transitions to the $^4T_{2g}$ and $^4T_{1g}$ states and the splitting of the ^2E_g state. The function minimized was

$$f = 10^3 S^2 + 10^2 \sum D^2 + \sum Q^2 \qquad (2)$$

where *S* in the first term is the ^2E_g splitting, and *D* and *Q* represent the differences between experimental and calculated $\{^2E_g, {}^2T_{1g}\}$ and $\{^4T_{2g}, {}^4T_{1g}\}$ transition energies, respectively. The Powell parallel subspace optimization procedure 20 was used to find the global minimum. The optimization was repeated several times with different sets of starting parameters to verify that the same global minimum was found. The results of the optimization and the parameter set used to generate the best-fit energies are also listed in Table 4. The fit is good for the ligand field transitions. The quartet terms were given a very low weight to reflect the very large uncertainty in their positions.

It is shown that the observed ^2E_g splitting, 102 cm^{-1} in the excitation spectrum can be reproduced by modern ligand field theory. We believe that the large extent of the distortion from orthoaxiality produces greater ^2E_g splitting than others. The higher energy $^4A_{2g} \rightarrow {}^2T_{2g}$ band was predicted at 22756 cm^{-1} from the calculation, but it could not be found in this region of solution absorption or solid ex-

Table 3. Optimized Cartesian and Spherical Polar Coordinates for Ligating Nitrogen Atoms in [Cr(*trans*-diammac)]$(ClO_4)_3$[a]

Atom	*x*	*y*	*z*	θ	ϕ
$N_{prim}(1)$	−0.1541	−0.1713	2.0542	6.40	−131.97
$N_{prim}(2)$	0.1541	0.1713	2.0542	173.60	48.03
$N_{sec}(1)$	2.0261	−0.0641	−0.1567	94.42	−1.81
$N_{sec}(2)$	0.0639	−2.0307	0.1736	85.12	−88.20
$N_{sec}(3)$	−2.0261	0.0641	0.1567	85.58	178.19
$N_{sec}(4)$	−0.0639	2.0307	−0.1736	94.88	91.80

[a]Cartesian coordinates in Å, polar coordinates in degrees.

Table 4. Experimental and Calculated Electronic Transition Energies for [Cr(*trans*-diammac)]$(ClO_4)_3$[a]

State(O_h)	Exptl	Calcd[b]
^2E_g	14700	14698
	14802	14796
$^2T_{1g}$	15237	15241
	15425	15517
	15620	15536
$^2T_{2g}$(avg)	?	22756
$^4T_{2g}$(avg)	23390	23736
$^4T_{1g}$(avg)	29980	29868

[a]Data in cm^{-1}. [b]$e_\sigma(N_{prim})=7542\pm85$, $e_\sigma(N_{sec})=8575\pm68$, $B=613\pm15$, $C=3161\pm30$, $\alpha_T=121\pm6$, $\zeta=270\pm20$.

citation spectra. An orbital population analysis yields a configuration of $(xy)^{0.95}(xz)^{1.01}(yz)^{0.99}(x^2\text{-}y^2)^{0.02}(z^2)^{0.02}$ for the lowest component of ^2E_g state. The relative *d*-orbital ordering from the calculations is $E(xy, xz)=0\ cm^{-1} < E(yz)=856\ cm^{-1} < E(x^2\text{-}y^2)=22882\ cm^{-1} < E(z^2)=25646\ cm^{-1}$. These factors can be used for predicting the photochemical reactivity of mixed-ligand chromium(III) complexes.[21] The following values were finally obtained for the ligand field parameters; $e_\sigma(N_{prim})=7542\pm85$, $e_\sigma(N_{sec})=8575\pm68$, $B=613\pm15$, $C=3161\pm30$, $T=121\pm6$, and $\zeta=270\pm20\ cm^{-1}$. The parameter values reported here appear to be rather significant, as deduced on the basis of a manifold of sharp-line transitions which were obtained from highly resolved excitation spectrum. The AOM parameters for *trans*-diammac indicate that the primary and secondary nitrogen atoms have very strong σ-donor properties toward chromium(III). The value of 7542 cm^{-1} for the $e_s(N_{prim})$ is comparable to 7505 cm^{-1} reported for $[Cr(en)_3]Cl_3$.[6] However, the value of 8575 cm^{-1} for the $e_s(N_{sec})$ parameter obtained from the complete ligand field analysis is the largest one among the values reported for nitrogen coordinated chromium(III) complexes. The result is in agreement with the shortest Cr-N bond length of 2.031 Å from X-ray crystal structure analysis.[17] The value of Racah parameter, *B* is only 66.8% of the value for a free chromium(III) ion in the gas phase. The ligand field parameters given here may be transferable to this type of other complexes as a basis for schematic analysis.

Acknowledgment. We wish to thank Professor Geoffrey A. Lawrance for a gift of the title compound. We also acknowledge financial support from the Dongil Research Foundation (1996).

References

1. (a) This is part 20 of the series *Electronic Structure and Chemical Reactivity of Transition Metal Complexes*; (b) The preceding publication in this series is Ref. 4.
2. Kirk, A. D.; Güdel, H. U. *Inorg. Chem.* **1992**, *31*, 4564.
3. Choi, J. H. *Bull. Korean Chem. Soc.* **1993**, *14*, 118.
4. Choi, J. H.; Oh, I. G.; Yeh, J. H. *Korean Appl. Phys.* **1996**, *9*, 722.
5. Kirk, A. D.; Hoggard, P. E.; Güdel, H. U. *Inorg. Chim. Acta* **1995**, *238*, 45.
6. Choi, J. H.; Lee, T. H. *Korean Appl. Phys.* **1994**, *7*, 186.
7. Hoggard, P. E. *Coord. Chem. Rev.* **1986**, *70*, 85.
8. Choi, J. H.; Oh, I. G. *Bull. Korean Chem. Soc.* **1993**, *14*, 348.
9. Choi, J. H. *J. Korean Chem. Soc.* **1995**, *39*, 501.
10. Choi, J. H. *J. Photosci.* **1996**, *3*, 43.
11. Hoggard, P. E. *Top. Curr. Chem.* **1994**, *171*, 114.
12. Lee, K. W.; Hoggard, P. E. *Inorg. Chem.* **1991**, *30*, 264.
13. Choi, J. H. *Bull. Korean Chem. Soc.* **1994**, *15*, 145.
14. Bernhardt, P. V.; Comba, P.; Hambley, T. W.; Lawrance, G. A. *Inorg. Chem.* **1991**, *30*, 942.
15. Bernhardt, P. V.; Comba, P.; Hambley, T. W.; Lawrance, G. A.; Várnagy, K. *J. Chem. Soc. Dalton Trans.* **1992**, 355.
16. Bernhardt, P. V.; Comba, P.; Hambley, T. W. *Inorg. Chem.* **1993**, *32*, 2804.
17. Bernhardt, P. V.; Comba, P.; Curtis, N. F.; Hambley, T. W.; Lawrance, G. A.; Maeder, M.; Siriwardena, A. *Inorg. Chem.* **1990**, *29*, 3208.
18. Trees, R. E. *Phys. Rev.* **1951**, *83*, 756.
19. Choi, J. H.; Hoggard, P. E. *Polyhedron* **1992**, *11*, 2399.
20. Kuester, J. L.; Mize, J. H. *Optimization Techniques with Fortran*; McGraw-Hill: New York, 1973.
21. Chung, J. J.; Hwang, J. U.; Choi, J. H. *J. Korean Chem. Soc.* **1986**, *30*, 181.

Ab initio Studies on d^8-$MCl(PH_3)_2(C_2H_2)$, M=Rh and Ir, Complexes

Sung Kwon Kang*, Jin Soo Song, Jung Hyun Moon, and Sock Sung Yun

Department of Chemistry, Chungnam National University, Taejon 305-764, Korea
(Received August 14, 1996)

The geometries and energies of the isomers in alkyne complexes $MCl(PH_3)_2(\eta^2\text{-}C_2H_2)$, M=Rh and Ir, are theoretically investigated using *ab initio* methods at the Hartree-Fock and up to MP4 level of theory and relativistic effective core potentials for Rh and Ir metals. The optimized structures of Rh complexes, **1-3** at MP2/ECP1 level are in good agreement with the related experimental data. The binding energies of C_2H_2 to d^8-metal fragments are computed to be ~55 kcal/mol. The vinylidene complexes for Rh and Ir metals are calculated to be much lower in energy than the alkyne complexes. The alkyne-vinylidene rearrangement is possible to proceed exothermically through the intermediate hydrido-alkynyl complexes, **2** or **9**. Detailed comparison is given about the geometries and relative energies on Rh and Ir isomers at the various level *ab initio* calculations with orbital analysis.

Introduction

The chemistry of unsaturated carbenes, such as vinylidene, allenylidene, and their derivatives which are coordinated to one or more transition metal fragments, has recently drawn substantial attention. Numerous examples of